RESEARCH ARTICLE | OCTOBER 06 2023

Innovative 3D-shaped structures as volumetric absorbers

Robin Tim Broeske; Peter Schwarzbözl; Lisa Birkigt; Sebastian Dung; Benedikt Müller; Till Doerbeck

AIP Conf. Proc. 2815, 100002 (2023)
https://doi.org/10.1063/5.0148829

Innovative 3D-Shaped Structures as Volumetric Absorbers

Robin Tim Broeske[1], Peter Schwarzbözl[1, a)], Lisa Birkigt[2], Sebastian Dung[3], Benedikt Müller[4], Till Doerbeck[4]

[1]*German Aerospace Center, Institute of Solar Research, Linder Höhe, 51147 Köln, Germany*
[2]*Exentis Technology GmbH, Otto-Schott-Straße 15, 07745 Jena, Germany*
[3]*Vitesco Technologies Emitec GmbH, Hauptstraße 128, 53797 Lohmar, Germany*
[4]*Kraftanlagen München GmbH, Ridlerstraße 31c, 80339 München, Germany*

[a)] Corresponding author: peter.schwarzboezl@dlr.de

Abstract. As proven by the continuous operation of the Solar Tower Juelich, central receiver power plants with open volumetric receivers are a valid alternative to other receiver types. Evolving new manufacturing techniques will allow to advance the technology further by improving its core component, the porous absorber structures. Using ceramic 3D screen printing, the new StepRec absorber design is fabricated out of siliconized silicon carbide and is presented along with the second new structure, the Emitec absorber made of very thin metal sheets. Based on experiments in the high-flux solar simulator Synlight, the thermal efficiency of both new designs is derived for reduced-size absorber probes. The new structures outperform the state-of-the-art HiTRec absorber with efficiencies above ninety percent at air temperatures of 650°C. Full-size absorber modules have been tested under real irradiation conditions at the research platform of the Solar Tower Juelich. The thermal efficiencies of the full modules will be quantified with further experiments in the Synlight facility in the near future.

INTRODUCTION

Open volumetric receivers present an alternative to the predominant molten salt or steam receivers for central receiver power plants. Integration of a heat storage is easier than for steam receivers, while the relative technical simplicity is advantageous to molten salt receivers as no heat tracing and no drainage during night-time is required. Commissioned in 2009, the Solar Tower Juelich proves the feasibility of a complete solar tower system with an open volumetric receiver [1]. The Juelich receiver deploys the so-called HiTRec receiver technology where the receiver is made up of thousands of small modules [2]. Each module incorporates a porous honeycomb absorber which absorbs the solar irradiation and heats the air flow. As a core component of open volumetric receivers, porous absorber structures have been an ongoing research topic with a more recent focus on 3D-shaped geometries. Such 3D-shaped absorbers are characterized by a purposefully varying geometry along the air flow direction. Important properties of the volumetric absorbers, e.g. the penetration depth of the incident solar irradiation, can be enhanced by the changing geometry leading to improvements of the absorber efficiency. Investigated 3D-shaped absorbers include layered ceramic foams [3,4,5], metal wire meshes [6], and absorbers created using additive manufacturing techniques [7,8].

ABSORBER GEOMETRIES

Two new absorber designs are presented, while the state-of-the-art HiTRec absorber design is used as the reference absorber. The HiTRec absorber used at the Solar Tower Juelich is a porous honeycomb absorber manufactured from extruded silicon carbide [2]. After extrusion, the absorber modules are infiltrated with additional silicon to yield the absorber material of siliconized silicon carbide (SiSiC). The heat conductivity and durability of the absorbers are improved by the infiltration. The HiTRec geometry consists of simple square channels with a constant channel width

SolarPACES: Solar Power & Chemical Energy Systems
AIP Conf. Proc. 2815, 100002-1–100002-8; https://doi.org/10.1063/5.0148829
Published by AIP Publishing. 978-0-7354-4623-6/$30.00

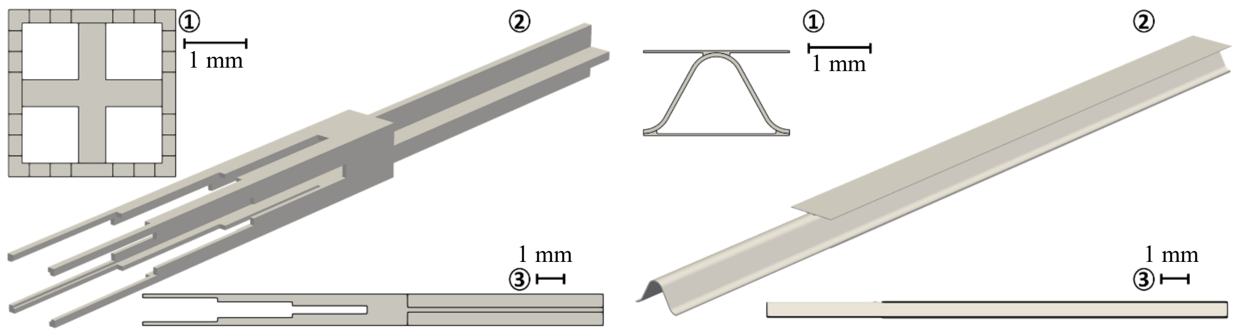

(a) (b)

FIGURE 1. Geometric unit cell models for the two new absorber designs: a) StepRec, b) Emitec (1: Front view, 2: 3D view, 3: Side view, views are pair-wise to scale)

of 2 mm and a wall strength of 0.8 mm [2]. The resulting porosity and specific surface area values are given in table 1. Wall strength refers to the material thickness perpendicular to the channel axis/air flow direction.

The first new StepRec absorber is an adaption of a design proposed by Capuano [8]. Each channel of the original design is characterized by thin pins at the irradiated absorber front. The width of the pins increases along the flow direction until the pin section is followed by a square channel section and a subsequent shifted square channel section. Using electron beam melting, only an upscaled (3:1) version out of a titanium aluminum alloy could be manufactured at the time of the design proposal [8]. For the new StepRec absorber, Capuano's design is adapted to the new manufacturing technique of ceramic 3D screen printing. This technology by the company Exentis Technology GmbH enables the production of a finer absorber out of the better suited absorber material of silicon carbide. Additionally, the new absorbers are also infiltrated with surplus silicon leading to an absorber material of SiSiC. The base channel width of 2.29 mm and wall strength of 0.44 mm correspond to a 2:1 upscaled version of Capuano's design. However, the sloped pins are replaced by three "step"-like sections for the new StepRec absorber as shown in the geometry model of a single absorber channel in figure 1a. This change is made necessary by the limitation of the 3D screen printing process, that every geometry change requires a new screen. The increasing pin width would therefore require endless screen changes. By replacing the pins with three steps, the StepRec absorbers are instead created using five distinct screens, one per step and one each for the base and shifted channel sections. Starting from a quarter of the channel width, the width of the step section doubles for each of the two subsequent steps mimicking the sloped pins. The small first pins give the StepRec absorber a high front porosity (94.5%) allowing for deeper penetration of the incident solar radiation. The porosity decreases with the successive absorber sections with the lowest value (70.3%) for the two square channel sections. Opposite, the specific surface area increases along the flow direction (cf. table 1).

The second new Emitec design is a steel membrane absorber manufactured by the company Vitesco Technologies Emitec GmbH. The absorber represents the continuation of a previous research collaboration [9]. Made possible by the continued development of the manufacturing technology, the new absorbers have a square shape, compared to the previous round and hexagonal shapes, increasing the compatibility to the HiTRec receiver technology. Each absorber is composed of alternating layers of curled and smooth metal sheets with a wall strength of 65 μm each. To increase the porosity at the absorber front, the smooth metal sheets were shortened such that the absorber front only contains curled sheets as shown in figure 1b. The small wall strength combined with the densely packed alternating metal layers results in a very fine absorber geometry (400 cpsi) with a high porosity and large specific surface area as listed in table 1.

Figure 2 compares 60 mm by 60 mm probes of the two new designs to a 68 mm by 68 mm HiTRec probe.

TABLE 1. Characteristic absorber properties. Porosity and surface area values are listed for each distinct absorber section ordered from the front to the back of each absorber. The values for the last two StepRec sections are identical.

Property	HiTRec	StepRec	Emitec
Absorber Material	SiSiC	SiSiC	Steel (FeCrAl, 1.4767)
Cells per Square Inch [cpsi]	80	87.5	400
Porosity Levels [-]	51.0%	94.5%; 86.5%; 78.4%; 70.3%	92.8%; 87.6%
Average Porosity [-]	51.0%	78.2%	88.9%
Specific Surface Area [m²/m³]	1020	367; 733; 1100; 1230	2230; 3200

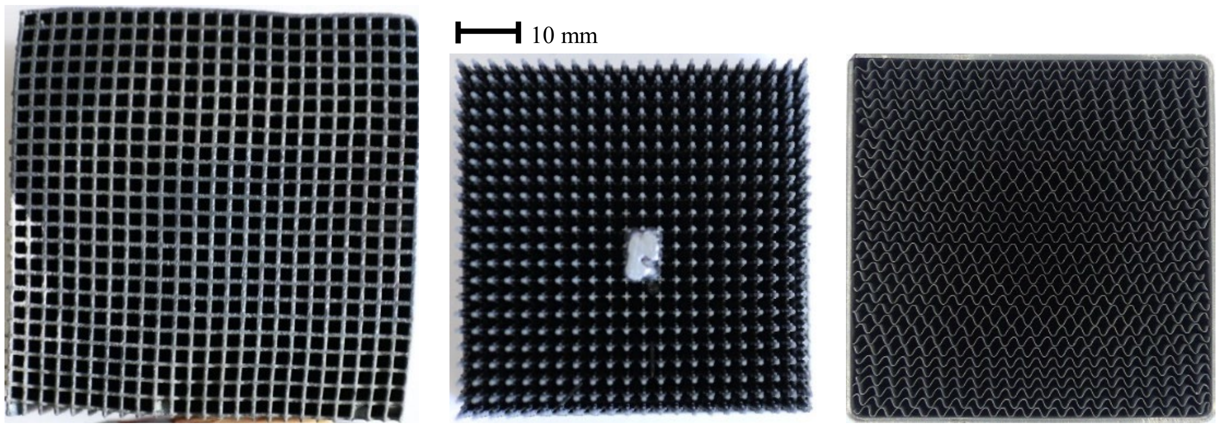

(a) (b) (c)

FIGURE 2. Front view of investigated volumetric absorbers: a) HiTRec, b) StepRec, c) Emitec

EXPERIMENTAL PERFORMANCE EVALUATION

In order to evaluate the new absorber geometries, experiments were conducted in the German Aerospace Center's high-flux solar simulator Synlight. The Synlight facility is located in Juelich, Germany and allows for experiments with an irradiation power of up to 310 kW [10]. The used test rig was built by Kraftanlagen München GmbH and is shown in figure 3. This setup allowed the parallel irradiation of sixteen 60mm by 60 mm absorber probes. Multiple different absorber geometries were assessed as part of the experimental campaign, from which the promising StepRec and Emitec absorbers were selected to be presented in this publication with the HiTRec absorber serving as the reference.

Data was recorded for two different irradiation levels. The average flux densities ranged from 327 kW/m² to 369 kW/m² for the lower level, and from 464 kW/m² to 535 kW/m² for the higher irradiation level. Data points were collected for varying air exit temperatures of up to 750°C. Three distinct absorber probes were available for the Emitec absorber, but only two for the StepRec geometry and one for HiTRec. To compensate, the HiTRec and StepRec probes were evaluated multiple times to yield three separate data sets per absorber geometry. As auxiliary experiments, reflection losses of each absorber probe were measured with a spectrometer. From the spectral reflection losses, solar-weighted absorptivity values were obtained for each absorber and are given in table 2. Due to oxidation, the metallic Emitec absorbers darkened during the irradiation in the Synlight facility. The reflection measurements were therefore conducted before and after the irradiation. Table 2 lists the values for the solar-weighted absorptivity after irradiation, which were up to one percentage point higher compared to before the irradiation for the Emitec probes.

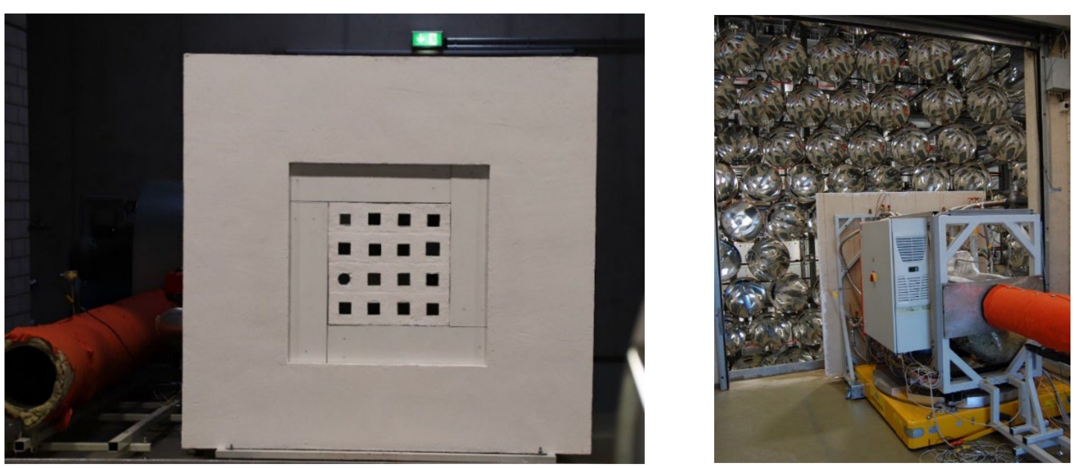

(a) (b)

FIGURE 3. Experimental test rig used for absorber performance evaluation: a) front view, b) rear view

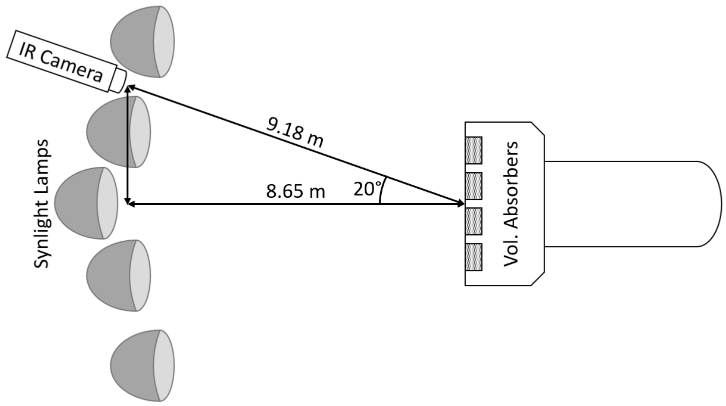

FIGURE 4. Schematic top-down view of the experimental setup: test rig with the volumetric absorbers on the right, infrared camera and Synlight lamps on the left (figure not to scale)

TABLE 2. Solar-weighted absorptivity for the three absorbers.

Absorber	**Solar-Weighted Absorptivity α_{sw}**
HiTRec	89.7%
StepRec	96.8% - 97.2%
Emitec	96.2% - 96.7%

During the experiments in the Synlight facility, thermal emissions of the absorber probes were recorded using an infrared camera. This camera was placed between the Synlight lamps viewing the test rig at an angle of around 20 degrees as can be seen in the schematic test setup overview of figure 4. From the infrared recordings, the thermal radiation losses per unit area $\dot{q}''_{r,loss}$ were derived for each absorber probe and air exit temperature T_{air}. The average incident flux density $I_0$was evaluated from measurements with DLR's FMAS system [11]. Combined with the solar-weighted absorptivity values α_{sw}, the thermal efficiency of the absorbers was then calculated as given by equation 1. The temporal development of the infrared measurements at the start-up and shutdown of the experiments, i.e. when the Synlight lamps were turned on/off, indicated that the infrared camera also captured reflections of the artificial irradiation along with the thermal emissions from the absorbers. To compensate, the reflections $\dot{q}''_{refl,IR}$ were estimated based on equation 2. The thermal efficiencies were extrapolated for air exit temperatures equal to the ambient temperature assuming that the efficiencies should asymptotically trend towards the solar-weighted absorptivity. The observed differences were then interpreted as the unintentionally measured reflections and rectified thermal efficiencies were defined by equation 3. This correction lead to efficiency increases ranging from 3.2 to 4.8 percentage points.

$$\eta_{th}(T_{air}) \coloneqq \alpha_{sw} - \frac{\dot{q}''_{r,loss}(T_{air})}{I_0} \quad (1)$$

$$\dot{q}''_{refl,IR} \coloneqq I_0\left(\alpha_{sw} - \eta_{th}^{extrapolation}(T_{amb})\right) \quad (2)$$

$$\eta_{th}^{rect}(T_{air}) \coloneqq \alpha_{sw} - \frac{\dot{q}''_{r,loss}(T_{air}) - \dot{q}''_{refl,IR}}{I_0} \quad (3)$$

Figure 5 presents the (rectified) thermal efficiency as a function of the air exit temperature for the three absorbers. The two new absorber designs clearly outperform the state-of-the-art HiTRec absorber for all air exit temperatures. At low temperatures, the thermal efficiency differences between the absorbers correspond to the different solar weighted absorptivities. The new absorbers also outperform the HiTRec geometry for high temperatures. At 650°C air exit temperature and the higher flux density levels (cf. Fig. 5b), efficiencies of 92.7%-93.7% for StepRec and 91.5%-92.5% (Emitec) are observed compared to 84.2%-85.2% for HiTRec.

In order to quantify the measurement error of the presented thermal efficiency results, the uncertainties of the different contributions to the thermal efficiency have to be assessed. For the evaluation of the solar-weighted absorptivities, the measuring process was specifically designed to minimize the influence of random measurement

(a)

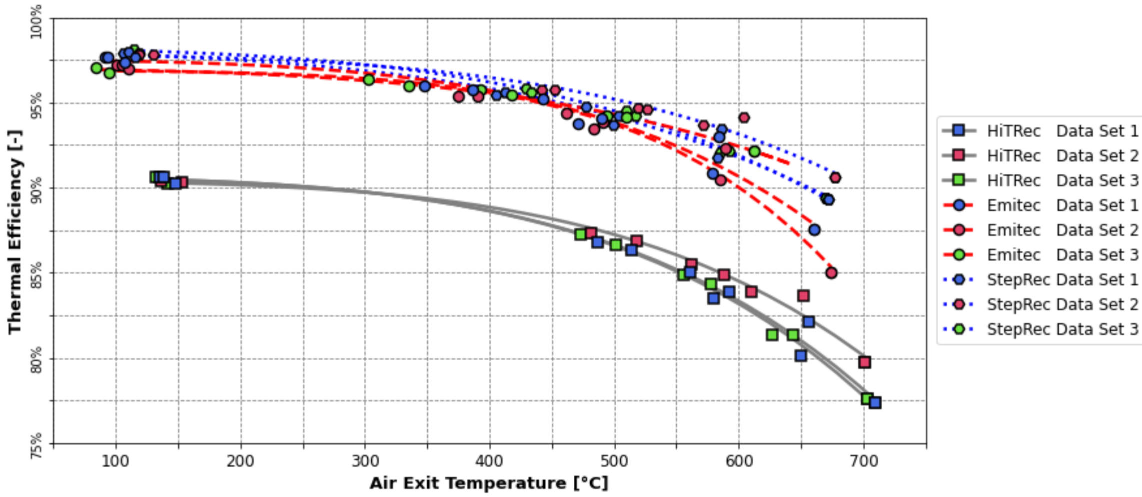

(b)

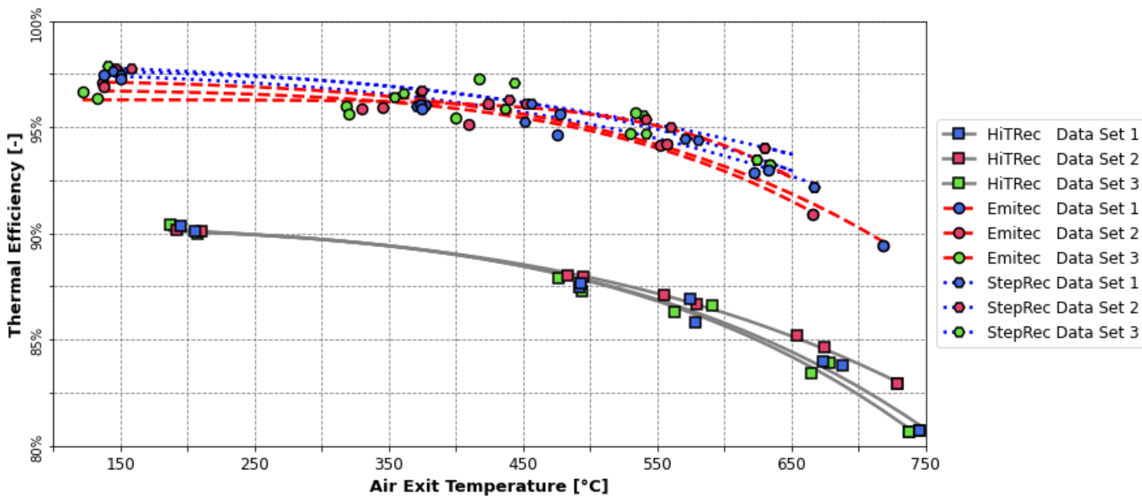

FIGURE 5. Thermal efficiency over air exit temperature for the experiments in the Synlight facility: a) lower irradiation levels (327 kW/m² - 369 kW/m²), b) higher irradiation levels (465 kW/m² - 535 kW/m²), markers represent data points, lines are least-square fits

errors. The analysis of the spectral reflectivity values with the spectrometer was repeated three times for each absorber probe. Each time, the absorber probe was rotated and/or moved, such that different sections of the absorbers were measured. Random errors caused by the spectrometer itself and by impurities in the absorber probes were reduced by this approach and are considered to be negligible. Before each series of reflectivity measurements, a reference plate with known spectral reflectivity was evaluated using the spectrometer. The spectral reflectivities of the absorbers were then calculated relative to the reference probe further negating possible measurement errors. Deviations of the emitted spectrum of the Synlight lamps from the solar spectrum, which was used to derive the solar-weighted absorptivities, were considered as a cause of a systematic error. However, their influence was deemed insignificant as the Synlight lamps have been specifically chosen for the application in a high-flux solar simulator. Differences w.r.t the angle of the incident radiation between the spectrometer measurements and the experiments in the Synlight were identified as another potential systematic error, but it was not possible to quantify this error at this time. Besides the previously mentioned infrared reflections (cf. equations 2 and 3), the positioning of the IR-camera, i.e. the angle dependency, and the used emissivities of the absorbers were identified as potential sources for uncertainty in the calculation of the emission losses. Both influences are currently being investigated in the lead-up to a second experimental campaign in the Synlight facility, but cannot be quantified at this point. The estimation of the infrared reflections can be viewed as an upper limit estimation, because the thermal efficiency will never fully reach the solar-weighted absorptivity even for very low air exit temperatures in reality. Therefore, the rectification $\dot{q}''_{refl,IR}$ is used as an uncertainty estimation for the emission losses. For the flux density measurements, a relative error between three and eight percent is expected based on experience from other experiments at DLR. As a conservative estimation, a relative error of ten percent is assumed for this experimental campaign. Using the reflectivity correction as the asymmetric (negative) error estimation for the emission losses and the symmetric relative error of the flux density measurement, an error propagation calculation was conducted. Table 3 shows the results for the higher flux density levels (cf. Fig. 5b) at an air exit temperature of 650°C. The uncertainty decreases for lower air exit temperatures as the emission losses also decrease. Also listed are the thermal efficiency ranges at 650°C to show that both new absorbers outperform the HiTRec absorber by a larger margin than the calculated error estimation. The difference between the two new absorbers has to be considered as indistinguishable w.r.t. the uncertainty.

TABLE 3. Error propagation estimation for the higher flux density levels (cf. Fig. 5b) at air exit temperatures of 650°C. (The efficiency rectification, cf. eqs. 2 & 3, are used as an asymmetric estimator for the uncertainty of the emission losses.)

Absorber	Rect. Th. Efficiency Range [%-Points]	Absolute Emission Error [%-Points]	Relative Flux Density Error [-]	Absolute Error Estimation [%-Points]
HiTRec	[84.2, 85.2]	[-3.9, 0]	[-10%, +10%]	[-4.9, +0.5]
StepRec	[92.7, 93.7]	[-3.8, 0]	[-10%, +10%]	[-4.7, +0.4]
Emitec	[91.5, 92.5]	[-3.6, 0]	[-10%, +10%]	[-4.5, + 0.4]

SCALE-UP AND DYNAMIC TESTS

Building on the presented results, the new absorber geometries have been scaled up to the standard 140 mm by 140 mm module size of the HiTRec receiver technology. The full-size absorber modules are shown in figure 6. Identical to the state-of-the-art HiTRec absorber modules, the full module is formed by combining the absorber matrix with a ceramic cup for the StepRec absorber. The first part of the absorber matrix spans the full 140 mm by 140 mm module width, while the size of remaining matrix is smaller in order to fit inside the ceramic cup. As a result, the absorber matrix shields the ceramic cup against direct irradiation. The upscaled version of the Emitec absorber is instead equipped with a metallic cup, which is welded directly onto the frame of the absorber matrix.

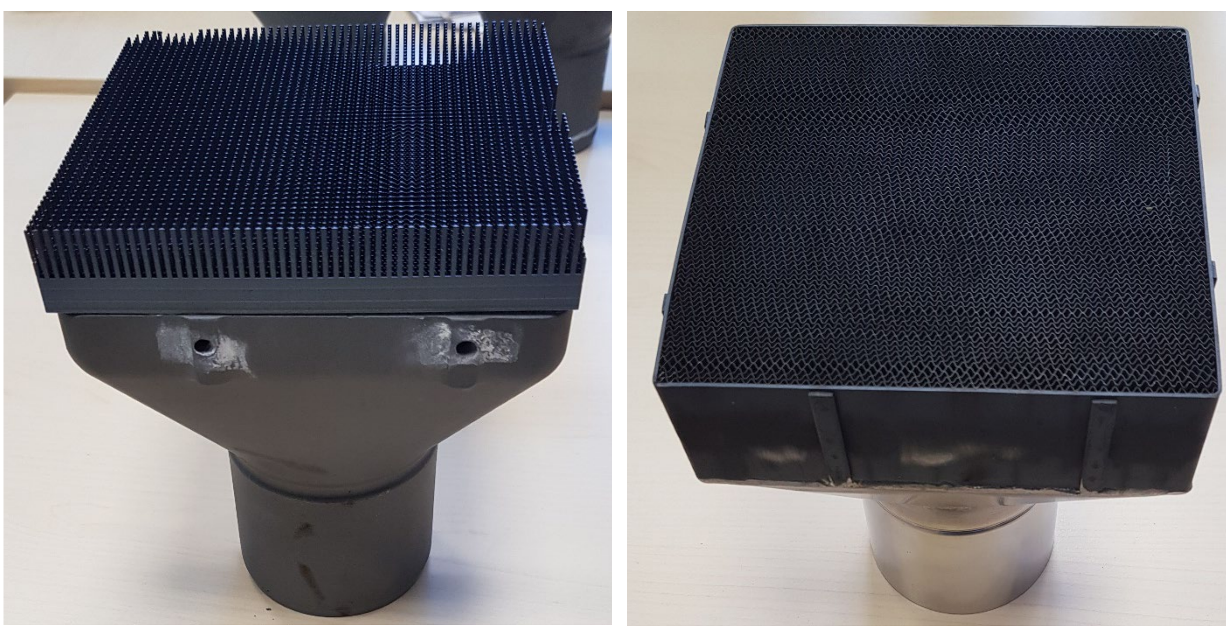

(a) (b)

FIGURE 6. Full-size absorber modules: a) StepRec, b) Emitec

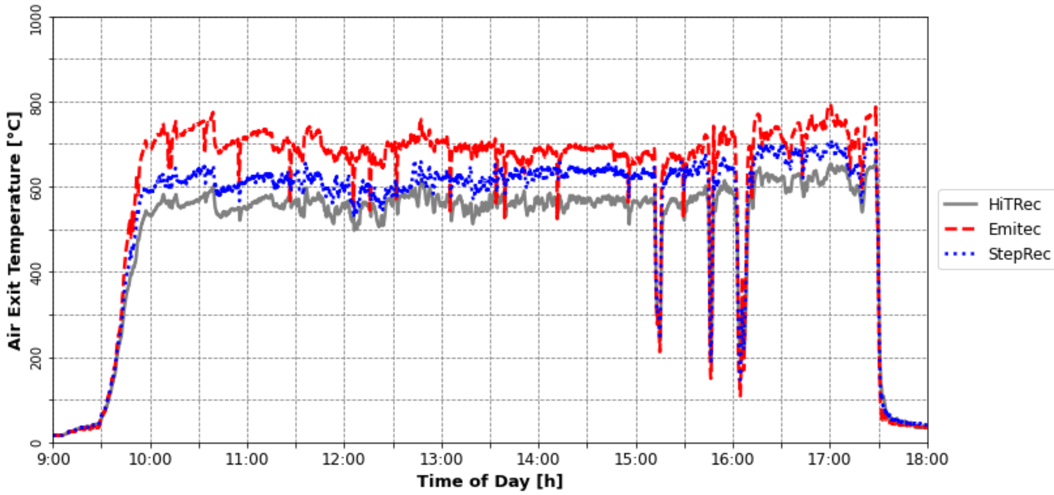

FIGURE 7. Air exit temperature over time for the experiments at the research platform of the Solar Tower Juelich for selected absorbers. Temperature drops caused by cloud passages can be observed between 15:00h and 16:30h. (Incident solar radiation varies between the three absorbers.)

At the research platform of the Solar Tower Juelich, experiments have been carried out to test the new full-size absorber modules under real irradiation conditions. In total, the new absorbers were successfully irradiated for 34 hours with flux densities of up to 700 kW/m². Figure 7 shows the absorber temperatures over the course of one example day of the conducted experiments. Multiple cloud passages during the afternoon caused significant drops in the absorber temperatures. Table 4 lists the maximum negative and positive air exit temperature gradients for the second cloud passage, which caused the strongest gradients. The temperature gradients for the absorber structures, in particular the absorber fronts, are expected to have been higher than the air exit temperature gradients. Nonetheless, the new absorbers withstood these sharp temperature gradients without any visible impact. Combined with the total irradiation duration, the dynamic conditions showed that the new absorbers are suitable for their application in open volumetric receivers.

TABLE 4. Maximum air exit temperature gradients caused by cloud passage (starting at 15:45h, cf. Fig. 7) during experiments at Solar Tower Juelich.

Absorber	Negative Gradient [K/min]	Positive Gradient [K/min]
HiTRec	-230	197
StepRec	-360	347
Emitec	-430	395

CONCLUSION

Two new porous absorber geometries for the use in open volumetric receivers for central tower power plants have been presented. The StepRec structure, is a 3D printed ceramic absorber out of SiSiC, while the Emitec absorber consists of a steel matrix formed by alternating smooth and curled metal sheets. For both new geometries, 60 mm by 60 mm probes have been successfully investigated experimentally in the Synlight facility. Thermal efficiencies over ninety percent are achieved by both designs at air exit temperatures of 650°C, clearly outperforming the reference state-of-the-art HiTRec absorber. Full-sized absorber modules have been manufactured and successfully tested under real irradiation conditions at the research platform of the Solar Tower Juelich. New experiments in the Synlight facility to measure the thermal efficiency of the full modules are planned to take place in the upcoming weeks. With numerical models, which are being developed at the German Aerospace Center, additional new absorber designs will be derived to take full advantage of the possibilities presented by the new manufacturing techniques.

ACKNOWLEDGMENTS

This work was supported by the German Federal Ministry for Economic Affairs and Energy on the basis of a decision by the German Bundestag, reference number 0324300B.

REFERENCES

1. Koll, G., Schwarzbözl, P., Hennecke, K., Hartz, T., Schmitz, M. and Hoffschmidt, B., *The Solar Tower Jülich - A Research and Demonstration Plant for Central Receiver Systems*. Proceedings of 15th SolarPACES Conference, 15 – 18 September 2009, Berlin, Germany (2009).
2. Hoffschmidt, B., Téllez, F. L. M., Valverde, A., Fernández, J. S. and Fernández, V., *Performance evaluation of the 200-kW$_{th}$ HiTRec-II open volumetric air receiver*. J. Sol. Energy Eng., **125**(1), 87-94 (2003).
3. Roldán, M.I., Smirnova, O., Fend, T., Casas, J.L., Zarza, E., *Thermal analysis and design of a volumetric solar absorber depending on the porosity*. Renewable Energy **62**, 116–128 (2014).
4. Chen, X., Xia, X.L., Meng, X.L., Dong, X.H., 2015. *Thermal performance analysis on a volumetric solar receiver with double-layer ceramic foam*. Energy Conversion and Management **97**, 282–289 (2015).
5. Zaversky, F., Aldaz, L., Sanchez, M., Ávila-Marín, A.L., Roldán, M.I., Fernández-Reche, J., Füssel, A., Beckert, W., Adler, J., *Numerical and experimental evaluation and optimization of ceramic foam as solar absorber – single-layer vs multi-layer configurations*. Applied Energy **210**, 351–375 (2018).
6. Ávila-Marín, A.L., Alvarez-Lara, M., Fernandez-Reche, J., *Experimental results of gradual porosity wire mesh absorber for volumetric receivers*. Energy Procedia **49**, 275-283 (2014).
7. Alberti, F., Santiago, S., Roccabruna, M., Luque, S., Gonzalez-Aguilar, J., Crema, L., Romero, M., *Numerical analysis of radiation propagation in innovative volumetric receivers based on selective laser melting techniques*. AIP Conference Proceedings **1734**, 030001 (2016), https://aip.scitation.org/doi/abs/10.1063/1.4949053.
8. Capuano, R., Fend, T., Stadler, H., Hoffschmidt, B., Pitz-Paal, R., *Optimized volumetric solar receiver: Thermal performance prediction and experimental validation*. Renewable Energy **114**, 556–566 (2017).
9. Pabst, C., Feckler, G., Schmitz, S., Smirnova, O., Capuano, R., Hirth, P., Fend, T., *Experimental performance of an advanced metal volumetric air receiver for solar towers*. Renewable Energy **106**, 91–98 (2017).
10. Wieghardt, K., Laaber, D., Dohmen, V., Hilger, P., Korber, D., Funken, K.H., Hoffschmidt, B., *Synlight - a new facility for large-scale testing in csp and solar chemistry*. Proceedings of the 23rd SolarPACES Conference, 26 – 29 September 2017, Santiago, Chile (2017).
11. Thelen, M., Raeder, C., Wilsch, C., Dibowski, H.-G., *A high-resolution optical measurement system for rapid acquisition of radiation flux density maps*. Proceedings of the 22nd SolarPACES Conference, 11 – 14 October 2016, Abu Dhabi, UAE (2016).